Real-time contrast medium detection in X-ray images by mathematical morphology operators

Dieu Sang Ly, Serge Beucher, Michel Bilodeau
MINES ParisTech, PSL - Research University, CMM - Centre for mathematical morphology, 35 rue St Honoré, 77300 Fontainebleau, France

Abstract. This article proposes a solution to contrast agent detection in angiograms by considering X-ray images as intensity images and applying mathematical morphology operators. We present two detection approaches, one based on the intensity infimum and the other based on the dual reconstruction. The evaluation using several data sets shows that both techniques are able to detect the presence of the contrast medium volume. Moreover, the dual reconstruction based method is proven to be faster in processing time and more effective than the intensity infimum based method in distinguishing the intensity change at the same location from the displacement of the same region. In addition, we show how to track the contrast agent passage through an ROI by observing the intensity evolution in successive sub-masks.

Keywords: contrast agent detection, contrast agent tracking, mathematical morphology, intensity infimum, dual reconstruction, x-ray.

Address all correspondence to: Dieu Sang Ly; E-mail: lydieusang@gmail.com

1 Introduction

Angiography is an imaging technique that uses a special dye and X-rays to visualize the inside of the arteries (such as the aorta), veins (such as the inferior vena cava) or organs of the body in the form of an angiogram. In the angiogram acquisition, a contrast material is injected into the patient through a thin tube (catheter) placed into a blood vessel, to facilitate the visualization of vascular structures. During the contrast material injection, the spiral diagnostic scans should be initiated properly in order to obtain the optimal contrast enhancement in the structure of interest. The most popular timing and synchronization techniques are fixed time-delay, bolus tracking and test bolus.[1]

- In the fixed time-delay technique, the diagnostic scans are initiated at a specified moment after the contrast material injection. This technique may be problematic in achieving the optimal contrast enhancement due to patient-related factors such as body size, cardiac output, cardiovascular circulation time.[2] Therefore, in order to better determine the scan timing, the

bolus tracking and test bolus techniques have been developed to monitor the contrast material bolus prior to the diagnostic scans. They predict the arrival of the contrast bolus at a specified location so that the acquisition can be synchronized with proper attenuation inside the region of interest (ROI).

- The bolus tracking technique starts with the acquisition of a pre-contrast scan, in which the ROI is placed on the blood vessel or organ of interest. The contrast medium bolus is then injected and a sequence of low-radiation-dose scans (monitor scans) are captured. At each sequential scan, the radiodensity within the ROI is computed and the time-attenuation curve is generated as illustrated in figure 1. When the contrast attenuation reaches a predefined trigger threshold, the monitor scans terminate and the diagnostic scans are initiated after an additional delay (diagnostic delay). The attenuation threshold and the diagnostic delay are two governing parameters of the bolus tracking technique.[3]

- In the test bolus technique, firstly, the test bolus (a small dose of the full contrast medium bolus) is injected and a series of low-radiation-dose images are acquired. At each scan, the contrast enhancement inside the ROI is measured and the time-attenuation curve is updated. This curve allows to determine the contrast material arrival time. Then the full bolus is injected and the diagnostic scans are triggered after the aforementioned contrast material arrival time[4] plus an additional delay.[5,6]

There exist several comparisons between the bolus tracking and test bolus techniques in *human tests*.[1,7–9] Cademartiri et al.[1] have shown that the bolus tracking technique results in better synchronization between the diagnostic scans and contrast material attenuation with a more homogeneous enhancement for coronary angiography. The bolus tracking requires shorter scanning

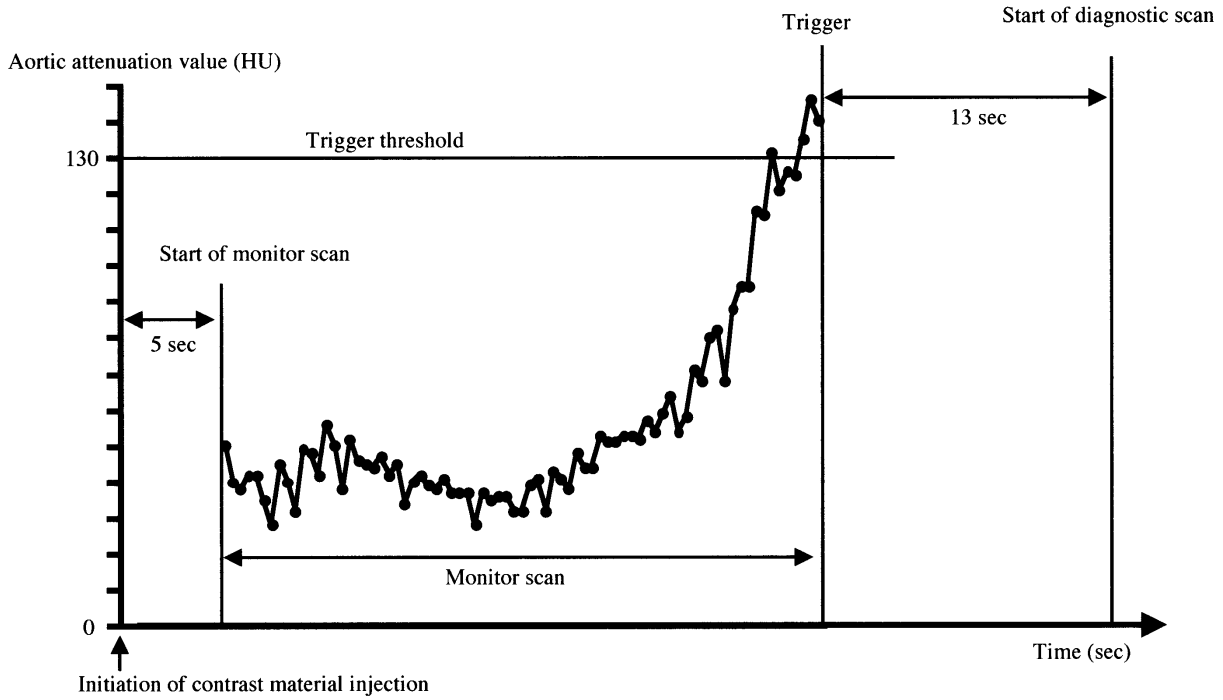

Fig 1 Time chart of bolus tracking technique[7]

time (hence less radiation exposure) and less contrast medium dose than the test bolus technique. On the other hand, the test bolus technique has the advantage that it is specifically adapted to the patient being examined and overcomes thus some limitations of the bolus tracking technique. For example, in the test bolus technique, the technologist can change the position of the ROI if misplacement occurs. Moreover, the test bolus technique allows to test the patient response, whether the heart rate remains steady or changes with breath holding during the contrast material injection.[3] The test bolus technique is preferable when performing short injection because the produced narrow maximal enhancement does not allow sufficient time for the bolus tracking to trigger and scan properly. Concerning *veterinary tests*, recent studies have also found that the bolus tracking has faster data acquisition and less contrast material volume than the test bolus technique for computed tomography angiography in healthy beagles[10] and cats.[11] The bolus tracking technique provides better synchronization between data acquisition and contrast medium passage.[11]

Both bolus timing techniques mentioned above monitor the contrast medium attenuation in HU (Hounsfield Units) which describes the radiopacity in a specific region. HU is a normalized value of the calculated attenuation coefficient of a pixel in a computed tomogram, based on a scale of -1000 (air) to +1000 (compact bone) with water being 0 and fat between -60 and -120. There are few works in the state of the art on bolus tracking using gray-level images. In,[12] the authors presented a real-time tracking of bolus propagation in leg vessels from X-ray angiograms. First, the vessel contrast is enhanced by a multi-scale adaptive enhancement method. Small vessels are enhanced much more than large vessels so that both types of vessels have similar opacity after the enhancement. At each scan, the bolus tracking is not performed directly on the contrast image but on two types of difference images: (i) the DSA image being the difference between the contrast image and the pre-contrast image acquired before the contrast medium injection and (ii) the DIFF image being the difference between the current and the previous contrast or DSA images. The acronyms DSA and DIFF are not expanded in the original paper. Next, the difference image is divided into a grid of N cells arranged along the predominant blood flow direction (vertical direction in this case) and a feature is extracted from this grid. DSA features describe the significance of dynamic information and DIFF features quantify the flow dynamics. A DSA or DIFF feature is an N-vector (or an N-sample curve), each element of which is the average of all pixels in the corresponding cell. Then, a curve fitting is applied. The peak of the DSA or DIFF feature corresponds to the cell where the bolus front is located. This peak localization allows to detect the arrival of the contrast material bolus at a predefined target region for gantry stepping. Dellandrea et al.[13] proposed to use active contours for bolus tracking in X-ray image sequences through four iterative steps. Firstly, the bolus region is identified in the first image by observing the intensity variation and its boundary is obtained by active contours. Secondly, the next location of the bolus

region is predicted by Kalman filter. Thirdly, the bolus region shape and position are optimized by a deformable region model and the bolus region boundary is refined by active contours. Lastly, the bolus motion is estimated and fed back to the Kalman filter. Recently, Li et al.[14] investigated the detection of non-calcified plaques of the coronary artery from the contrast-enhanced computed tomography angiograms. The detection starts with the segmentation of three-dimensional coronary tree by classifying voxels based on their attenuation. In other words, voxels with the attenuation higher than 160 HU (value obtained from their bibliographical research and own experiments) are detected inside the lumen. On the contrary, the attenuation outside the lumen is less than 160 HU. In addition, region growing is applied to fill holes and obtain the lumen boundary. Next, the centreline of the 3D coronary tree is extracted from its segmentation. Then, a voxel-map based on mathematical morphology is generated in order to structurally and quantitatively analyse coronary artery walls on the 3D coronary tree model, which allows to identify the plaque type and location.

In this work, we propose a solution to contrast material bolus detection and tracking by considering X-ray produced images as gray-level images and using mathematical morphology operators as the core of our algorithm. According to our best knowledge, this is the first work on automatic contrast agent detection using mathematical morphological operators. In clinical units, the arrival of the contrast agent is observed in real time by a technologist and then the acquisition of the spiral diagnostic scans is initiated manually. We propose two detection methods and prove that the second one, based on dual reconstruction, can deal with the affect of patient movement. The rest of the article is organised as follows: sections 2 and 3 describe our technique of contrast agent detection and tracking; section 4 presents some experimental results and section 5 concludes the paper.

2 Contrast agent detection by mathematical morphology operators

When X-ray images are processed as gray-scale images, their mean intensity normally descends with the invasion of the contrast agent (CA) as shown in figure 2. The pre-contrast frame is usually selected to be the reference frame. In the ideal case when the reference and current frames are different uniquely in intensity, a given location in the current frame is occupied by the CA if and only if its intensity in the current frame is inferior to that in the reference frame. Therefore, the first solution to detect the CA is based on the **intensity infimum** between the reference and current frames. However, the patient being examined rarely remains immobile, the detection by intensity infimum returns not only the presence of the contrast material but also the moving regions in the image. We propose thus another solution, based on a geodesic operator of mathematical morphology called **geodesic dual reconstruction**,[15] to extract the intensity difference at the same location rather than the movement of the same location. The definition of geodesic reconstruction and dual reconstruction is given below and illustrated by figure 3. The contrast agent detection based on intensity infimum and dual reconstruction is described by one-dimensional images in figure 4.

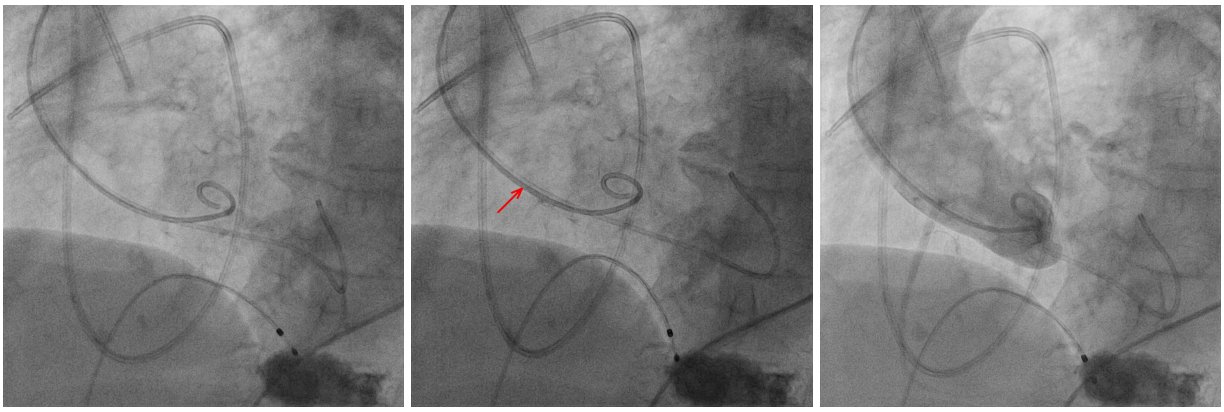

Fig 2 X-ray images with the contrast agent arrival. Left: pre-contrast image. Middle: contrast agent first appears in the catheter marked by red arrow. Right: contrast agent invades the aortic root. The image intensity decreases with the contrast agent arrival.

Definitions

The reconstruction **R** of a function g by a function f (supposing $g \geq f$) is the supremum of n successive geodesic dilations of f under g (see figure 3 - left).

$$\mathbf{R}_g(f) = \vee\{\delta_g^{(n)}(f)\} \tag{1}$$

The dual reconstruction **R*** of a function g by a function f (supposing $f \geq g$) is the infimum of n successive geodesic erosions of f above g (see figure 3 - right).

$$\mathbf{R}^*_g(f) = \wedge\{\epsilon_g^{(n)}(f)\} \tag{2}$$

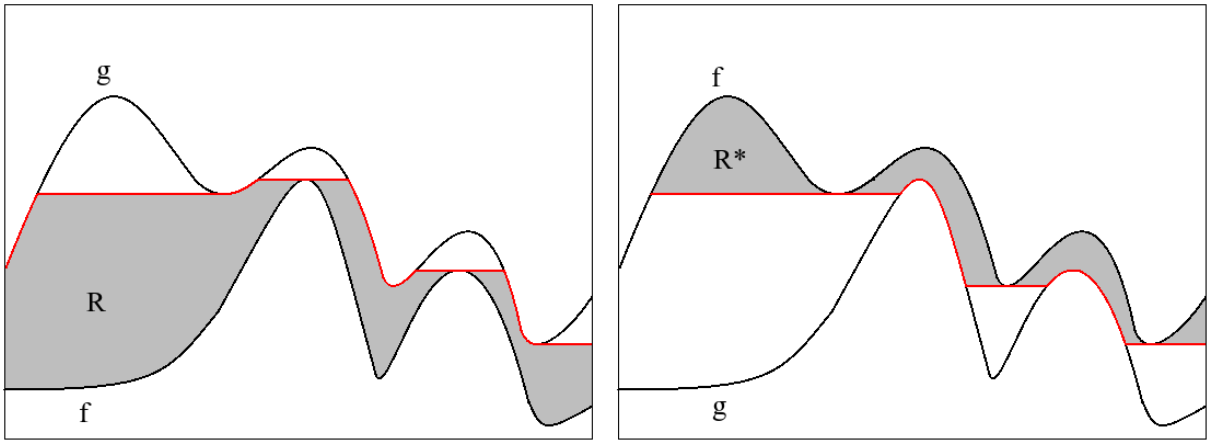

Fig 3 Geodesic reconstruction and dual reconstruction. Left: Successive dilations (in gray) of f under g result in the reconstruction **R** of g by f (in red). Right: Successive erosions (in gray) of f above g result in the dual reconstruction **R*** of g by f (in red).

General steps of two proposed CA detection methods are presented and compared in table 1 and their intermediate results are shown in figure 5.

- The pre-filtering step of the CA detection by intensity infimum consists of morphological closing and opening.[16] The closing operator (dilation followed by erosion) fills small back-

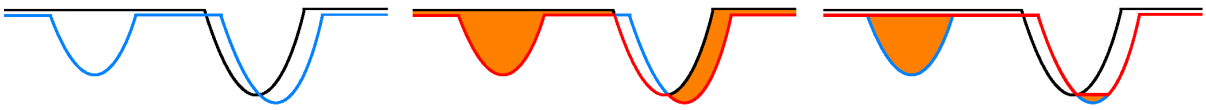

Fig 4 Contrast agent detection illustrated in one-dimensional images. Left: reference frame in black and contrast frame in blue. Middle: contrast agent detection by intensity infimum. The intensity infimum of two frames is in red; the difference between the intensity infimum and the reference frame in orange shows not only the intensity descent by the presence of contrast material (left orange region) at the same location but also possibly the movement of the same location (right orange region). Right: contrast agent detection by dual reconstruction. The dual reconstruction of the current frame by the reference frame is in red; the difference between the dual reconstruction and the current frame in orange shows the negative peaks of the current frame inferior to the reference frame; we can see that it emphasizes the intensity descent at the same location (left orange region) rather than the movement of the same location (small right orange region).

ground holes and the opening operator (erosion followed by dilation) removes small details of foreground objects. Whereas the dilation and erosion affect all regions of pixels indiscriminately, the closing and opening are less destructive of original boundary shape. In our experiments, the pre-filtering step was not required in the CA detection by dual reconstruction, making this method more advantageous than the CA detection by intensity infimum as the pre-filtering modifies the original content of the images.

- Steps 2 and 3 extract the contrast material bolus in the current frame. Note that in the first approach, one can also compute the intensity supremum between the current and reference frames, and then the difference between the intensity supremum and the current frame. As the current frame intensity is not always lower than the reference frame intensity, the dual reconstruction of the current frame by the reference frame is the infimum of the successive geodesic erosions of the supremum of two frames above the current frame.

- The post-filtering step, which consists of closing, opening and area opening, is used to eliminate small undesired detected regions. Another drawback of the CA detection by intensity infimum resides in this post-filtering as in some cases, this method does not discriminate

well the intensity change at the same location and the movement of the same location as the CA detection by dual reconstruction does (see the illustration in figure 4).

CA detection by intensity infimum	**CA detection by dual reconstruction**
1. Pre-filter the reference and current frames	1. *No need of pre-filtering*
2. Compute the intensity infimum between the current and reference frames	2. Build the dual reconstruction of the current frame by the reference frame
3. Compute the difference between the intensity infimum and the reference frame, and threshold this difference	3. Compute the difference between the dual reconstruction and the current frame, and threshold this difference
4. Post-filter	

Table 1 Contrast agent detection by intensity infimum and dual reconstruction

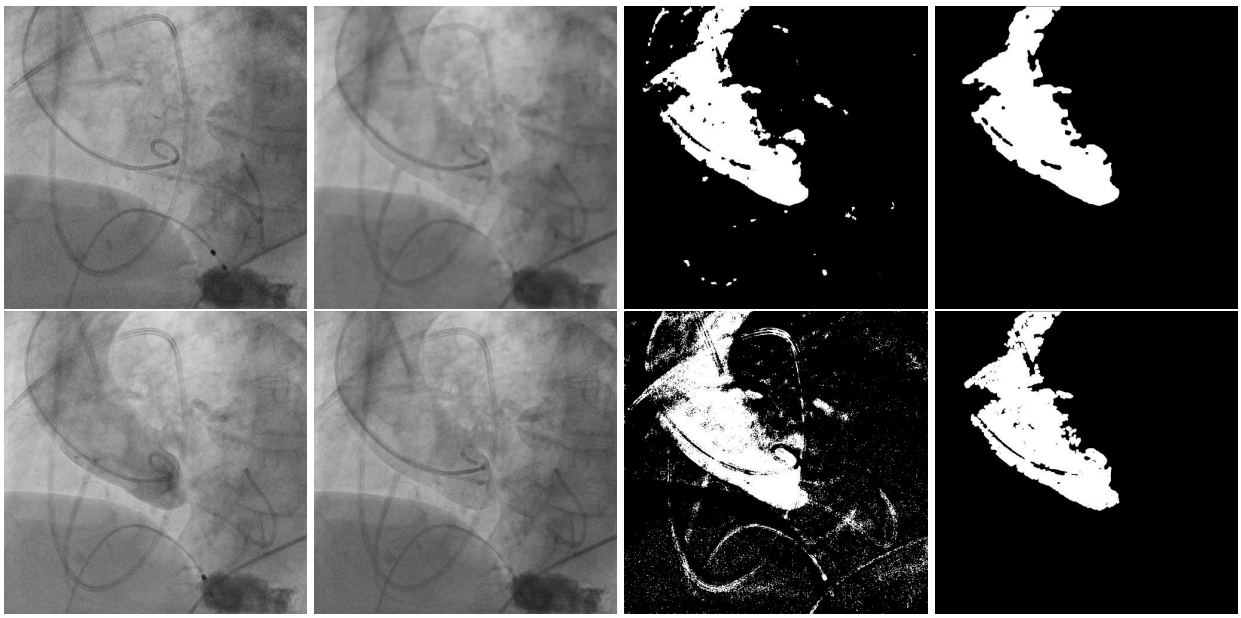

Fig 5 Intermediate results of two contrast agent detection approaches. Column 1: reference (upper) and current (lower) frames. Column 2: intensity infimum between the pre-filtered current and reference frames (upper) and dual reconstruction of the current frame by the reference frame (lower). Column 3: difference between the intensity infimum and the pre-filtered reference frame (upper) and difference between the dual reconstruction and the current frame (lower). Column 4: results after the post-filtering. The top-left part of the contrast material bolus is not detected because the corresponding region does not differ in intensity between the reference and current frames.

3 Contrast agent tracking using ROI mask

In some case, the ROI mask is available for the contrast material monitoring. The contrast medium detection technique described in the previous section can be performed under the ROI mask. In

order to track the movement of the contrast medium bolus in the structure of interest, we divide the ROI mask into adjacent sub-masks. For the sake of simplicity, the division is done horizontally as illustrated in figure 6. The mean intensity of the contrast image under all sub-masks is observed simultaneously during the CA injection. We will show in the experimental results that this observation allows to track the contrast agent passage through the ROI and may be used to determine the triggering moment of the diagnostic scans.

Fig 6 X-ray image with it ROI mask and the division of ROI mask into sub-masks. Left: pre-contrast image of the ascending aorta and catheter for the contrast agent injection. Middle: mask of the ascending aorta obtained by the 2D projection of its 3D reconstruction. Right: mask divided horizontally into 5 sub-masks with similar height.

4 Experimental results

In this section we present the results of our proposed contrast agent detection approaches using several X-ray sequences listed in table 2.

Sequence title	Frame dimension	Number of frames
Aorta01	118x118 mm (1016x1016)	56
Aorta02	115.85x115.85 mm (1016x1016)	60
Aorta03	216.50x216.50 mm (1024x1024)	223
Aorta04	174.41x174.41 mm (1024x1024)	88
Heart	194.56x194.56 mm (1024x1024)	40

Table 2 Sequences of X-ray images

- The sequences “Aorta01” to “Aorta04” are captured in the transcatheter aortic valve implantation (TAVI) procedure, the purpose of which is to implant an artificial aortic valve inside the patient’s own aortic valve without open heart surgery. The main event in these sequences is that the contrast agent enters the ascending aorta via a catheter and goes down the descending aorta.

- The sequence “Heart” is shot roughly at the starting point of the rotational scan in order to image the abdomen. The main event in this sequence is that the contrast agent arrives in the large vein from lower body and travels through the heart following the cardiac cycle.

4.1 Comparison between contrast agent detection approaches based on intensity infimum and dual reconstruction

In this section, we compare two methods of contrast medium detection proposed in section 2 using sequences “Aorta01”, “Aorta02” and “Heart” listed in table 2. In each sequence, a pre-contrast frame which is not so distant from the frame in which the CA enters the catheter is selected to be the reference frame in order to discard the abundant observation and to reduce the influence of patient’s movement during the acquisition. In practice, the reference frame can be chosen by the technologist according to the moment of injecting the contrast material. In other words, the technologist observes the CA movement in real time and may select the closest moment to the CA arrival in the region of interest as the reference frame.

Sequences “Aorta01” and “Aorta02”

Figures 7 and 8 show the detected contrast medium bolus at different moments of each sequence. The two proposed techniques provided quite similar results. However, the dual reconstruction based approach is likely to suppress the detection along the catheter caused by the displace-

ment of the catheter whereas the intensity infimum based approach can not discard this undesired detection. This result is conformable to the explanation in figure 4.

Concerning the computation time, the dual reconstruction based method is much faster than the intensity infimum based one. Without program optimization, the dual reconstruction based method requires about 60 milliseconds per frame whereas the intensity infimum based method requires about 100 milliseconds per frame. This duration includes the loading of current frame, four steps of the detection described in table 1 and the display of detection results.

Sequences "Heart"

Figure 9 illustrates the contrast material detection in different frames of this sequence. With frame #00 being the reference frame, the results from two proposed methods are presented in rows 3 and 4 of this figure. The results are indifferent between two techniques. They show the passage of the contrast medium bolus through the heart: #19 the CA enters the right atrium and ventricle from the inferior vena cava, #24 the CA is pumped up to the pulmonary veins, #34 the CA returns back to the left atrium and ventricle, #39 the CA is pumped up to the ascending aorta.

Concerning the computation time, the dual reconstruction based approach is much less time consuming than the intensity infimum based one. The average processing time for each frame is 120 milliseconds by the dual reconstruction method and 230 milliseconds by the intensity infimum one. The processing time for "Heart" is in general higher than that for "Aorta01" and "Aorta02" as the structuring elements of morphological operators used for "Heart" are bigger than those used in "Aorta01" and "Aorta02".

In the same figure, row 5 illustrates the detection by dual reconstruction based approach using frame #07 as the reference frame. The detection for contrast frames #19, #24 and #39 using #07

as reference frame is similar to that using #00 as reference frame. However, using reference frame #07 shows that in frame #34, the CA is also present in the ascending aorta.

4.2 Contrast agent detection and tracking using ROI mask

In this section, we evaluate the dual reconstruction based method of contrast material detection with and without ROI mask using sequences "Aorta03" and "Aorta04" listed in table 2.

Figure 10 shows the contrast agent detection in different frames of sequence "Aorta03" with and without using ROI mask. This result shows that the contrast medium bolus is injected to the the aortic root through the catheter, pumped up to the ascending aorta and then travels down the descending aorta. Similarly, figure 11 presents the detection result for sequence "Aorta04". From this result, we can see that the contrast material does not pass through the aorta in the same manner as it does in sequence "Aorta03", but seems to enter and exit the aorta in several cycles. For example, from frames #53 to #58, whereas a bolus leaves the upper part of the ascending aorta, another bolus enters the lower part of the ascending aorta.

In order to further investigate the contrast agent injection, we track its displacement through the ROI mask. We first divide the ROI mask into consecutive sub-masks. Next, we monitor simultaneously the intensity evolution in each sub-mask throughout the sequence. This is similar to generate the time-attenuation curve by measuring the radiodensity (in HU) of a particular location, except that we deal with mean intensity in gray-scale image. Figure 12 shows the measured intensity in individual sub-masks of sequence "Aorta03". The unique global minimum in each curve shows that the CA passed through each sub-mask region only once and continuously. Each intensity curve is denoted by 2 moments: the curve starting to descend (CA entering the sub-mask region) and starting to ascend (CA leaving the sub-mask region). The appearance order of these moments

(red → green → blue → magenta → cyan) along the sequence corresponds to the displacement of the CA through consecutive sub-masks (0 to 4). Similarly, figure 13 illustrates the mean intensity in each sub-mask of sequence "Aorta04". Several minima of each curve (e.g. 3 minima of the red curve) show that the CA was injected discontinuously. The CA displacement can be observed in 3 phases, each of which starts when CA enters sub-mask 0 (red curve starts to descend) and ends when CA leaves sub-mask 0 (red curve starts to ascend). The injection is composed of 3 cycles that we mark by the orange windows: #20 to #30, #35 to #47, #53 to #63. The inter-cycles illustrate the CA displacement: CA leaves sub-mask 0 (red curve ascends) and enters sub-masks 1 and 2 (blue and green curves descend). This can be seen clearly for sub-masks 0 (red curve) and 2 (blue curve) as they are the first and last sub-mask regions (in other words, the beginning and the end of the CA passage in the ROI), whereas it is less obvious for sub-mask 1 (green curve) as it is the intermediate sub-mask region.

5 Conclusion and discussion

We have proposed a solution to contrast agent detection in angiograms by processing X-ray produced images as intensity images. The proposed detection techniques based on intensity infimum and dual reconstruction have been evaluated with several X-ray image sequences. Compared to the intensity infimum based method, the dual reconstruction based one is more effective in distinguishing the intensity change at the same location from the displacement of the same region and faster in computation time. The latter is promising to be executed in real-time. We also presented how to track the contrast agent passage through an ROI by monitoring the intensity evolution in consecutive sub-masks. To the best of our knowledge, this is the first work on CA detection using mathematical morphological operators, which may be used in real-time application and can deal

with the patient displacement during image acquisition. It may be necessary to carry out a further study on the determination of triggering moment based on the time-intensity curves of the sub-masks. A possible extension of this work is to consider an adaptive division of the ROI mask into sub-masks along its centreline, which may improve the accuracy of the contrast agent tracking. In

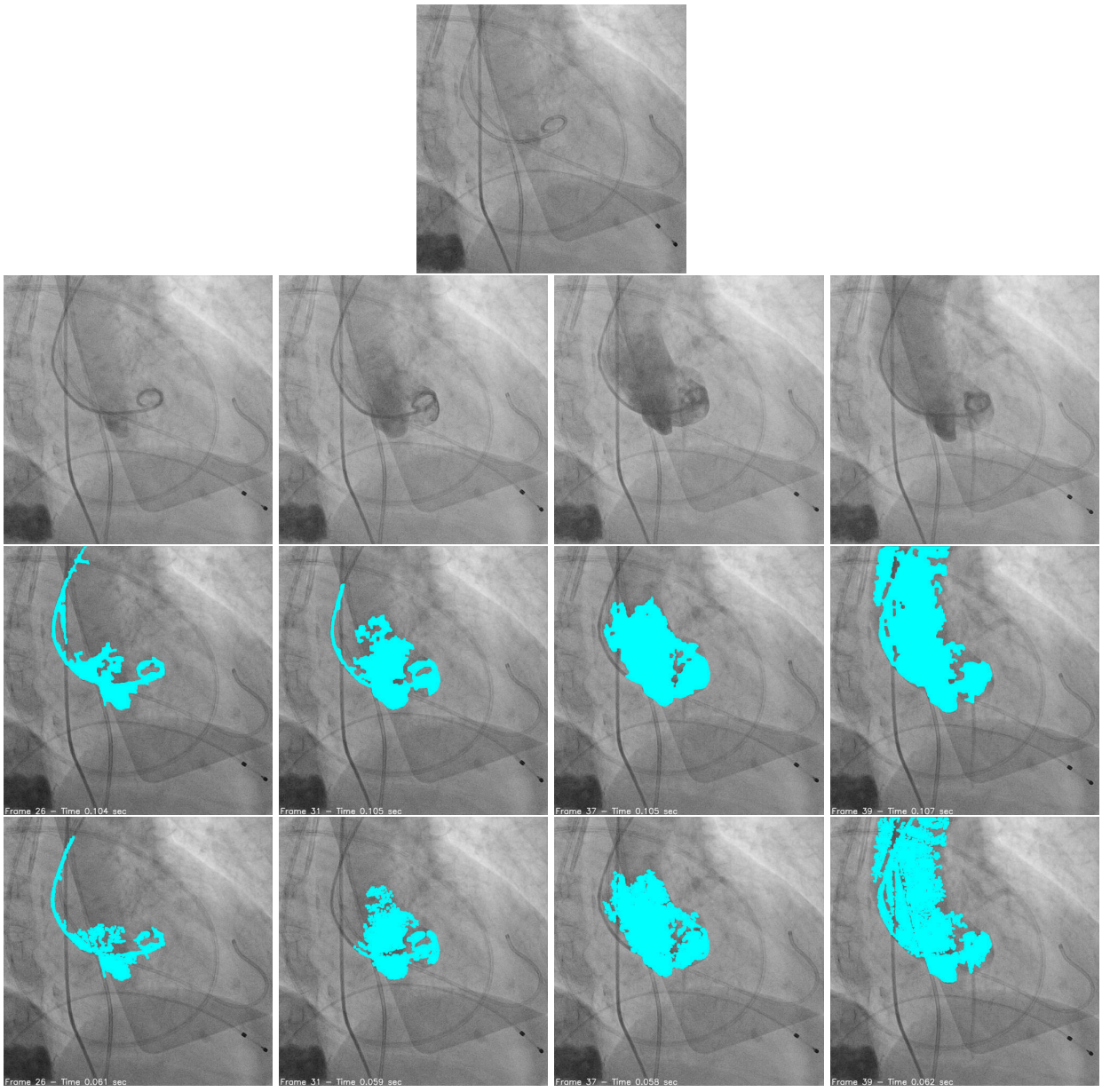

Fig 7 Contrast agent detection in sequence "Aorta01". Row 1: reference frame (#20). Row 2: contrast frames (#26, #31, #37 and #39 from left to right) showing the invasion of the contrast agent in the ascending aorta. Row 3: CA detection for corresponding frames in row 2 by intensity infimum. Row 4: CA detection for corresponding frames in row 2 by dual reconstruction

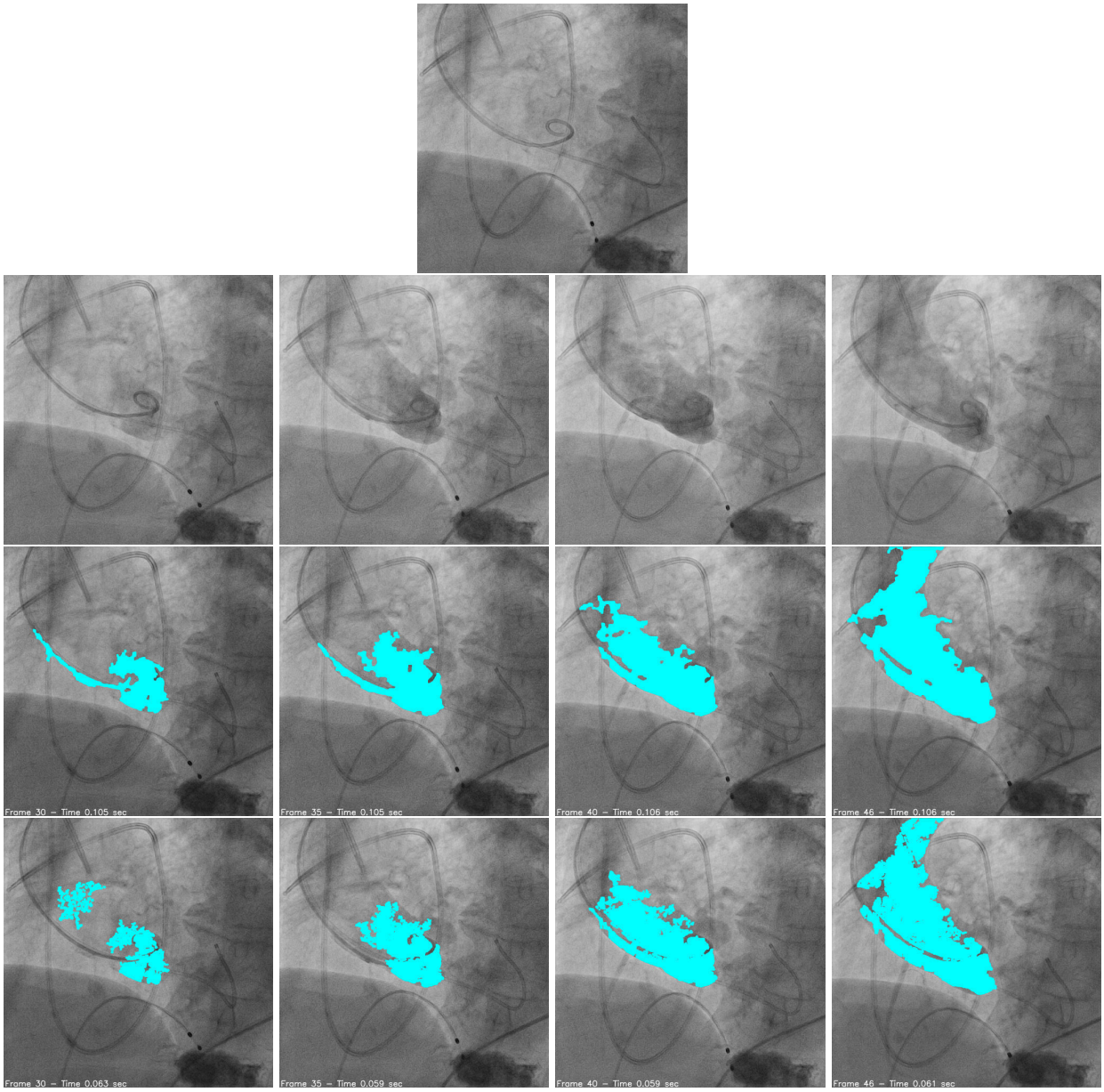

Fig 8 Contrast agent detection in sequence "Aorta02". Row 1: reference frame (#22). Row 2: contrast frames (#30, #35, #40 and #46 from left to right) showing the invasion of the contrast agent in the ascending aorta. Row 3: CA detection for corresponding frames in row 2 by intensity infimum. Row 4: CA detection for corresponding frames in row 2 by dual reconstruction. The top-left region of the contrast medium bolus in frame #46 is not detected because the intensity at that location remains unchanged as compared to the reference frame.

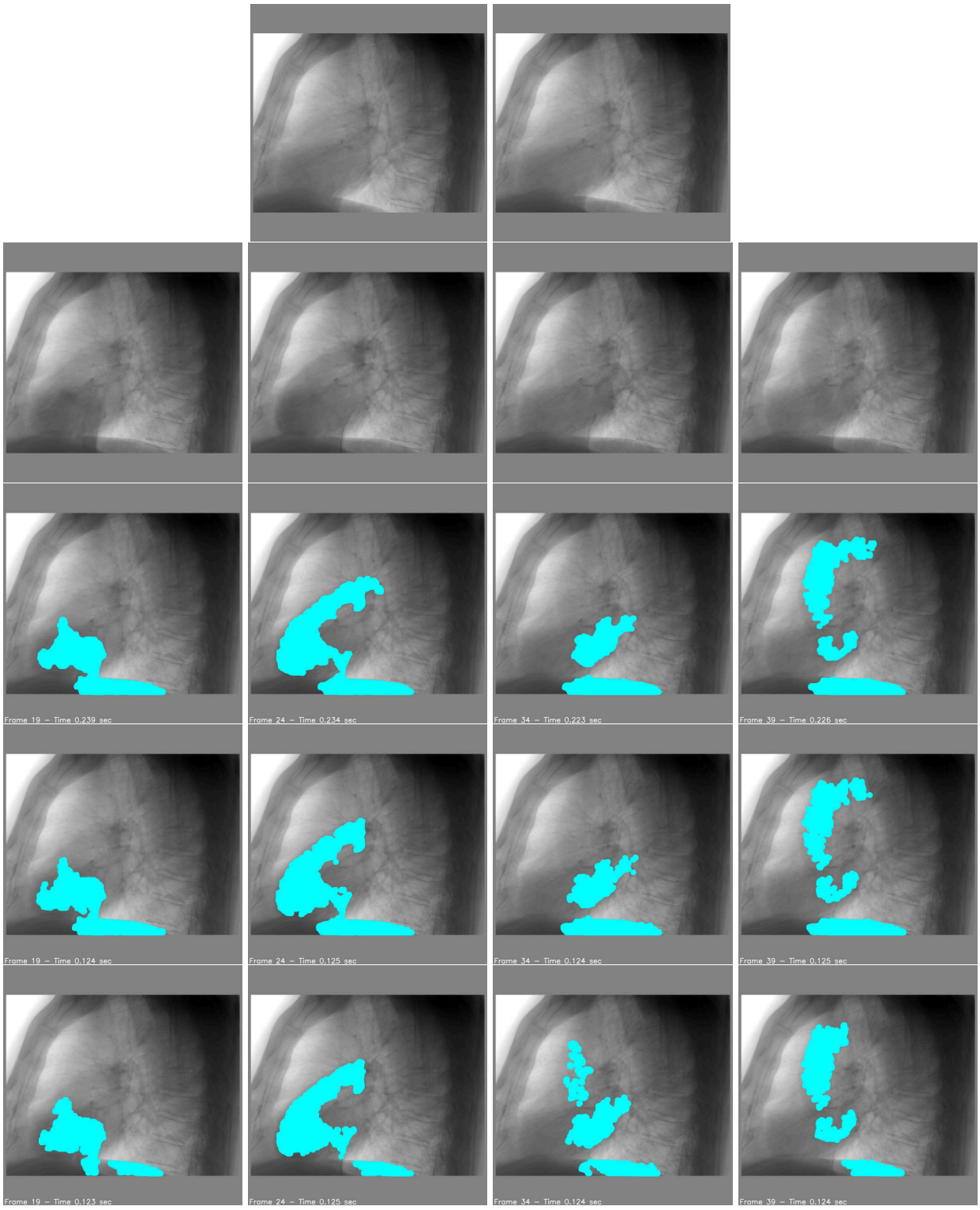

Fig 9 Contrast agent detection in sequence "Heart". Row 1: reference frames (#00 left and #07 right). Row 2: contrast frames (#19, #24, #34 and #39 from left to right). Row 3: CA detection for corresponding frames in row 2 by intensity infimum using #00 as reference frame. Row 4: CA detection for corresponding frames in row 2 by dual reconstruction using #00 as reference frame. Row 5: CA detection for corresponding frames in row 2 by dual reconstruction using #07 as reference frame.

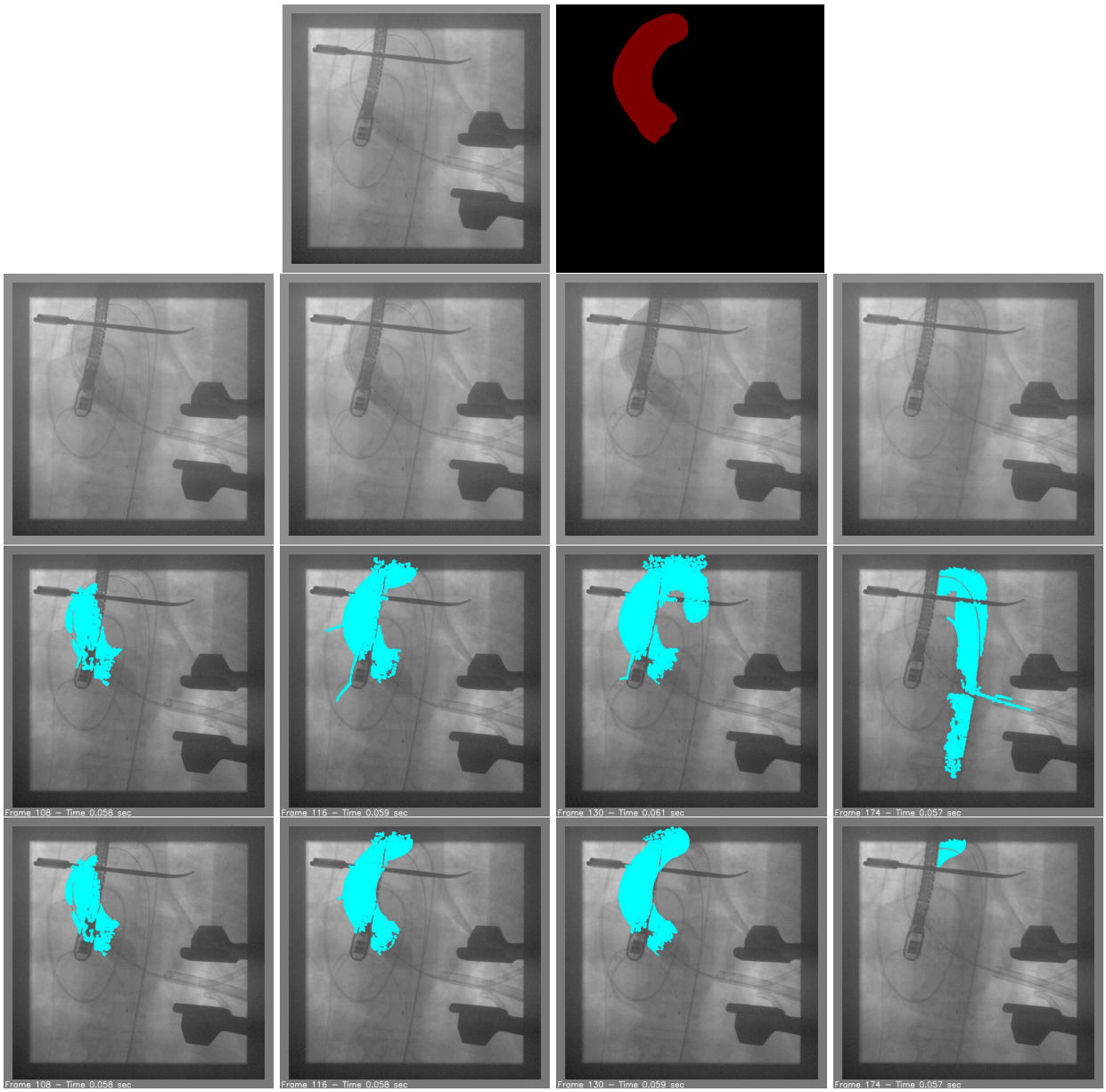

Fig 10 Contrast agent detection in sequence "Aorta03". Row 1: reference frame (#93) and the ROI mask. Row 2: contrast frames (#108, #116, #130 and #174 from left to right) showing the displacement of the CA in the aorta. Row 3: CA detection for corresponding frames in row 2 by dual reconstruction without ROI mask. Row 4: CA detection for corresponding frames in row 2 by dual reconstruction with ROI mask.

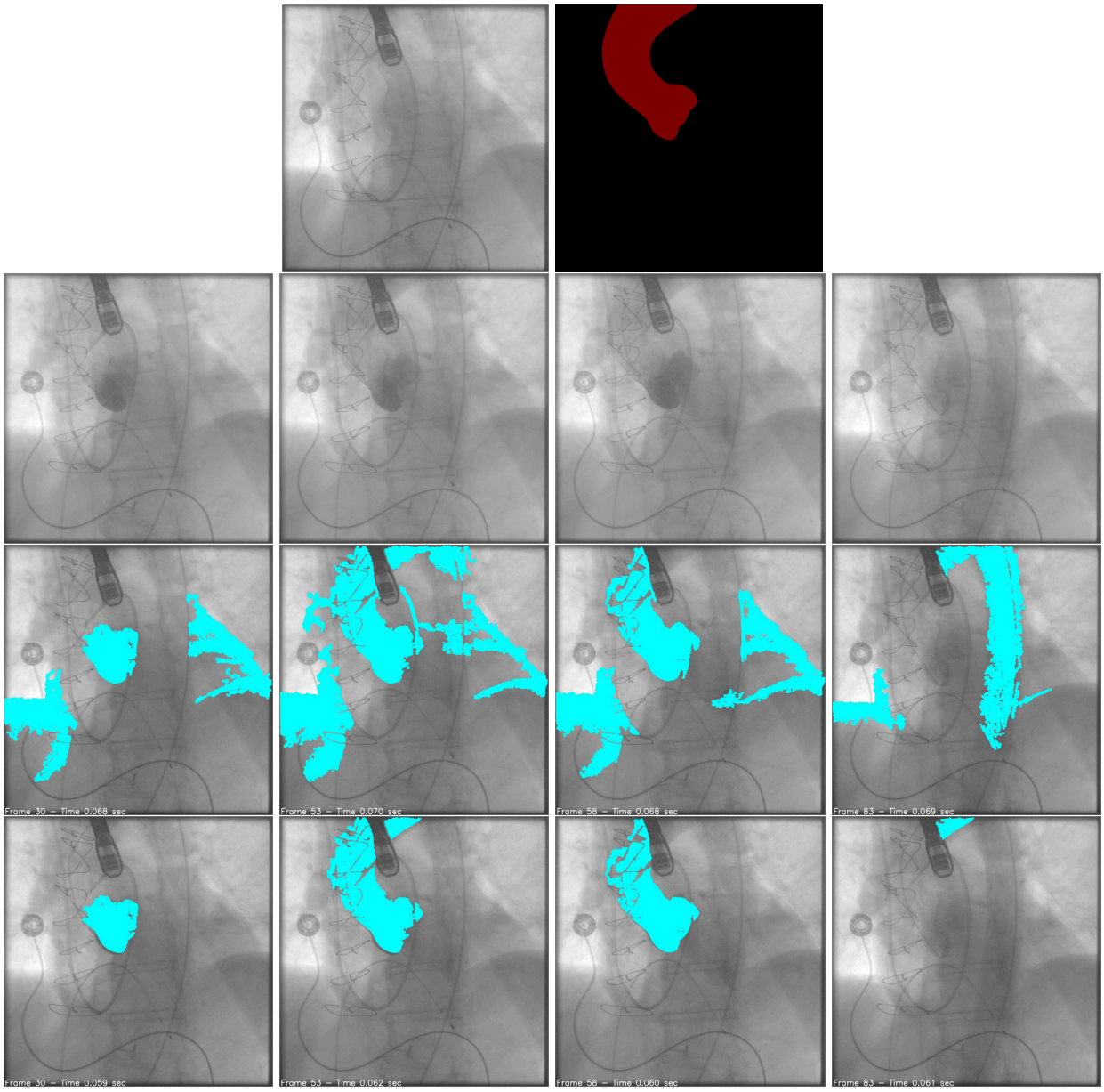

Fig 11 Contrast agent detection in sequence "Aorta04". Row 1: reference frame (#00) and the ROI mask. Row 2: contrast frames (#30, #53, #58 and #83 from left to right) showing the displacement of the contrast agent in the aorta. Row 3: CA detection for corresponding frames in row 2 by dual reconstruction without ROI mask. Row 4: CA detection for corresponding frames in row 2 by dual reconstruction with ROI mask.

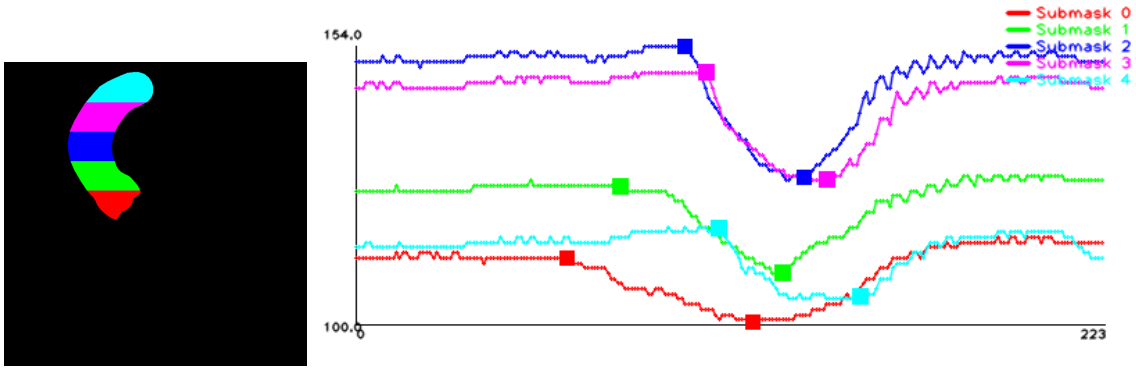

Fig 12 Mean intensity in each sub-mask along the sequence "Aorta03": x-axis: frame index, y-axis: mean intensity

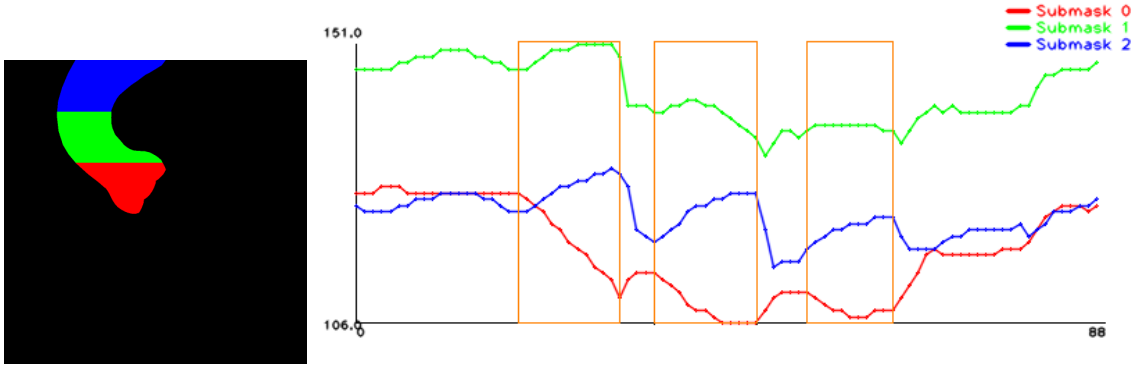

Fig 13 Mean intensity in each sub-mask along the sequence "Aorta04": x-axis: frame index, y-axis: mean intensity

addition, due to the patient's movement, the provided ROI mask may not encompass the regions occupied by the contrast material. Therefore, after the contrast agent detection in each contrast frame, it may be possible to adjust the original ROI mask by mathematical morphology operators to ensure that the final mask best fits the detected contrast medium bolus.

Acknowledgments

This work has been performed in the project PANORAMA, co-funded by grants from Belgium, Italy, France, the Netherlands, and the United Kingdom, and the ENIAC Joint Undertaking.

References

1 F. Cademartiri, K. Nieman, A. van der Lugt, R. Raaijmakers, N. Mollet, P. Pattynama, P. de Feyter, and G. Krestin, "Intravenous contrast material administration at 16-detector

row helical ct coronary angiography: test bolus versus bolus-tracking technique," *Radiology* **233**(3), 817–823 (2004).

2 A. Adibi and A. Shahbazi, "Automatic bolus tracking versus fixed time-delay technique in biphasic multidetector computed tomography of the abdomen," *Iran J Radiol* **11**(1), e4617 (2014).

3 K. T. Bae, "Intravenous contrast medium administration and scan timing at ct: Considerations and approaches," *Radiology* **256**, 32–61 (2010).

4 R. Sheiman, V. Raptopoulos, P. Caruso, T. Vrachliotis, and J. Pearlman, "Comparison of tailored and empiric scan delays for ct angiography of the abdomen," *American Journal of Roentgenology* **167**(3), 725–729 (1996).

5 K. Bae, "Peak contrast enhancement in ct and mr angiography: When does it occur and why? pharmacokinetic study in a porcine model," *Radiology* **227**(3), 809–816 (2003).

6 D. Fleischmann, "High-concentration contrast media in mdct angiography: Principles and rationale," *European Radiology* **13**(SUPPL. 3), N39–N43 (2003).

7 S. Itoh, M. Ikeda, M. Achiwa, H. Satake, S. Iwano, and T. Ishigaki, "Late-arterial and portal-venous phase imaging of the liver with a multislice ct scanner in patients without circulatory disturbances: Automatic bolus tracking or empirical scan delay?," *European Radiology* **14**(9), 1665–1673 (2004).

8 M.-J. Kim, E. Yong, W. Ki, J.-J. Chung, S. Joon, T. Young, and H. Joo, "Variation of the time to aortic enhancement of fixed-duration versus fixed-rate injection protocols," *American Journal of Roentgenology* **186**(1), 185–192 (2006).

9 T. Henzler, M. Meyer, M. Reichert, R. Krissak, J. W. N. Jr., S. Haneder, S. O. Schoenberg, and

C. Fink, "Dual-energy {CT} angiography of the lungs: Comparison of test bolus and bolus tracking techniques for the determination of scan delay," *European Journal of Radiology* **81**(1), 132 – 138 (2012).

10 N. Cassel, A. Carstens, and P. Becker, "The comparison of bolus tracking and test bolus techniques for computed tomography thoracic angiography in healthy beagles," *Journal of the South African Veterinary Association* **84**(1) (2013).

11 W. Mai, J. Suran, A. Cceres, and J. Reetz, "Comparison between bolus tracking and timing-bolus techniques for renal computed tomographic angiography in normal cats," *Veterinary Radiology and Ultrasound* **54**(4), 343–350 (2013).

12 Z. Wu and J.-Z. Qian, "Real-time tracking of contrast bolus propagation in x-ray peripheral angiography," in *Proceedings of the IEEE Workshop on Biomedical Image Analysis*, *WBIA '98*, 164–171, IEEE Computer Society, (Washington, DC, USA) (1998).

13 E. Dellandrea, P. Makris, M. Boiron, and N. Vincent, "Active contours for bolus tracking in x-ray images sequences," in *MVA*, 303–306 (2000).

14 Y. Li, W. Chen, K. Liu, Y. Wu, Y. Chen, C. Chu, B. Fang, L. Tan, and S. Zhang, "A voxel-map quantitative analysis approach for atherosclerotic noncalcified plaques of the coronary artery tree," *Computational and Mathematical Methods in Medicine* **2013** (2013).

15 S. Beucher and F. Meyer, "The morphological approach to segmentation: the watershed transformation," *Optical Engineering* **34**, 433–481 (1993).

16 P. Soille, *Morphological Image Analysis: Principles and Applications*, Springer-Verlag New York, Inc., Secaucus, NJ, USA, 2 ed. (2003).

Dieu Sang Ly is research engineer at Mines ParisTech, PSL - Research University. He received the B.Eng. degree in Electrical-Electronics Engineering from the University of Technology, Ho Chi Minh City, Vietnam in 2006; the M.Sc. degree in Computer Vision and Robotics from the Erasmus Mundus program in 2008 and the Ph.D. degree in Computer Vision from University of Picardie Jules-Verne, Amiens, France in 2011. His main research interests include camera modeling, image feature extraction, structure from motion and image processing with mathematical morphology.

Serge Beucher, PhD, is research director at PSL Research Institute (Paris School of Mines) and project leader for ARMINES. His professional interests have included segmentation techniques in image analysis, design of image analysers, development of morphological software on various platforms, real-time applications (on-board vision systems), industrial quality control by vision. His current research include image segmentation, computer vision, analysis of 3D scenes and image understanding.

Biographies and photographs of the other authors are not available.

List of Figures

List of Tables